Dual-comb modelocked lasers: semiconductor saturable absorber mirror decouples noise stabilization

Sandro M. Link,* Alexander Klenner, and Ursula Keller

Department of Physics, Institute for Quantum Electronics, ETH Zürich, 8093 Zürich, Switzerland
**slink@phys.ethz.ch*

Abstract: In this paper we present the stabilization of the pulse repetition rate of dual-comb lasers using an intracavity semiconductor saturable absorber mirror (SESAM) for passive modelocking and an intracavity birefringent crystal for polarization-duplexing to obtain simultaneous emission of two modelocked beams from the same linear cavity sharing all components. Initially surprising was the observation that the cavity length adjustments to stabilize one polarization did not significantly affect the pulse repetition rate of the other. We gained insight in the underlying physics using both a semiconductor and Nd:YAG laser gain material with the conclusion that the pulse arrival timing jitter of the two beams is decoupled by the uncorrelated time delay from the saturated SESAM and becomes locked with sufficient but not too much pulse overlap. Noise stabilization is in all cases still possible for both combs. The dual-comb modelocked laser is particularly interesting for the semiconductor laser enabling the integration of gain and absorber layers within one wafer (referred to as the modelocked integrated external-cavity surface emitting laser - MIXSEL).

OCIS codes: (140.3425) Laser stabilization; (140.4050) Mode-locked lasers; (140.5960) Semiconductor lasers; (140.7090) Ultrafast lasers; (260.1440) Birefringence.

References and links

1. D. Cotter, "Technique for highly stable active mode-locking," in *Ultrafast Phenomena IV* (Monterey, 1984), pp. 78–80.
2. M. J. W. Rodwell, D. M. Bloom, and K. J. Weingarten, "Subpicosecond laser timing stabilization," IEEE J. Quantum Electron. **25**(4), 817–827 (1989).
3. A. Schlatter, B. Rudin, S. C. Zeller, R. Paschotta, G. J. Spühler, L. Krainer, N. Haverkamp, H. R. Telle, and U. Keller, "Nearly quantum-noise-limited timing jitter from miniature Er:Yb:glass lasers," Opt. Lett. **30**(12), 1536–1538 (2005).
4. H. R. Telle, G. Steinmeyer, A. E. Dunlop, J. Stenger, D. H. Sutter, and U. Keller, "Carrier-envelope offset phase control: A novel concept for absolute optical frequency measurement and ultrashort pulse generation," Appl. Phys. B **69**(4), 327–332 (1999).
5. D. J. Jones, S. A. Diddams, J. K. Ranka, A. Stentz, R. S. Windeler, J. L. Hall, and S. T. Cundiff, "Carrier-envelope phase control of femtosecond mode-locked lasers and direct optical frequency synthesis," Science **288**(5466), 635–639 (2000).
6. A. Apolonski, A. Poppe, G. Tempea, C. Spielmann, T. Udem, R. Holzwarth, T. W. Hänsch, and F. Krausz, "Controlling the phase evolution of few-cycle light pulses," Phys. Rev. Lett. **85**(4), 740–743 (2000).
7. V. Gerginov, C. E. Tanner, S. A. Diddams, A. Bartels, and L. Hollberg, "High-resolution spectroscopy with a femtosecond laser frequency comb," Opt. Lett. **30**(13), 1734–1736 (2005).
8. J. Mandon, G. Guelachvili, and N. Picqué, "Fourier transform spectroscopy with a laser frequency comb," Nat. Photonics **3**(2), 99–102 (2009).
9. T. Steinmetz, T. Wilken, C. Araujo-Hauck, R. Holzwarth, T. W. Hänsch, L. Pasquini, A. Manescau, S. D'Odorico, M. T. Murphy, T. Kentischer, W. Schmidt, and T. Udem, "Laser frequency combs for astronomical observations," Science **321**(5894), 1335–1337 (2008).
10. D. Hillerkuss, R. Schmogrow, T. Schellinger, M. Jordan, M. Winter, G. Huber, T. Vallaitis, R. Bonk, P. Kleinow, F. Frey, M. Roeger, S. Koenig, A. Ludwig, A. Marculescu, J. Li, M. Hoh, M. Dreschmann, J. Meyer,

#253662 Received 9 Nov 2015; revised 18 Jan 2016; accepted 19 Jan 2016; published 25 Jan 2016

S. Ben Ezra, N. Narkiss, B. Nebendahl, F. Parmigiani, P. Petropoulos, B. Resan, A. Oehler, K. Weingarten, T. Ellermeyer, J. Lutz, M. Moeller, M. Huebner, J. Becker, C. Koos, W. Freude, and J. Leuthold, "26 Tbit s^{-1} line-rate super-channel transmission utilizing all-optical fast Fourier transform processing," Nat. Photonics **5**(6), 364–371 (2011).
11. D. Hillerkuss, R. Schmogrow, M. Meyer, S. Wolf, M. Jordan, P. Kleinow, N. Lindenmann, P. C. Schindler, A. Melikyan, X. Yang, S. Ben-Ezra, B. Nebendahl, M. Dreschmann, J. Meyer, F. Parmigiani, P. Petropoulos, B. Resan, A. Oehler, K. Weingarten, L. Altenhain, T. Ellermeyer, M. Moeller, M. Huebner, J. Becker, C. Koos, W. Freude, and J. Leuthold, "Single-laser 32.4 Tbit/s Nyquist WDM transmission," J. Opt. Commun. Netw. **4**, 715–723 (2012).
12. F. Keilmann, C. Gohle, and R. Holzwarth, "Time-domain mid-infrared frequency-comb spectrometer," Opt. Lett. **29**(13), 1542–1544 (2004).
13. A. Schliesser, M. Brehm, F. Keilmann, and D. van der Weide, "Frequency-comb infrared spectrometer for rapid, remote chemical sensing," Opt. Express **13**(22), 9029–9038 (2005).
14. S. Schiller, "Spectrometry with frequency combs," Opt. Lett. **27**(9), 766–768 (2002).
15. I. Coddington, W. C. Swann, and N. R. Newbury, "Coherent multiheterodyne spectroscopy using stabilized optical frequency combs," Phys. Rev. Lett. **100**(1), 013902 (2008).
16. B. Bernhardt, A. Ozawa, P. Jacquet, M. Jacquey, Y. Kobayashi, T. Udem, R. Holzwarth, G. Guelachvili, T. W. Hänsch, and N. Picqué, "Cavity-enhanced dual-comb spectroscopy," Nat. Photonics **4**(1), 55–57 (2010).
17. A. Bartels, R. Cerna, C. Kistner, A. Thoma, F. Hudert, C. Janke, and T. Dekorsy, "Ultrafast time-domain spectroscopy based on high-speed asynchronous optical sampling," Rev. Sci. Instrum. **78**(3), 035107 (2007).
18. K. O. Hill, Y. Fujii, D. C. Johnson, and B. S. Kawasaki, "Photosensitivity in optical fiber waveguides: Application to reflection filter fabrication," Appl. Phys. Lett. **32**(10), 647 (1978).
19. S. M. Link, A. Klenner, M. Mangold, C. A. Zaugg, M. Golling, B. W. Tilma, and U. Keller, "Dual-comb modelocked laser," Opt. Express **23**(5), 5521–5531 (2015).
20. D. J. H. C. Maas, A.-R. Bellancourt, B. Rudin, M. Golling, H. J. Unold, T. Südmeyer, and U. Keller, "Vertical integration of ultrafast semiconductor lasers," Appl. Phys. B **88**(4), 493–497 (2007).
21. U. Keller, K. J. Weingarten, F. X. Kärtner, D. Kopf, B. Braun, I. D. Jung, R. Fluck, C. Hönninger, N. Matuschek, and J. Aus der Au, "Semiconductor saturable absorber mirrors (SESAMs) for femtosecond to nanosecond pulse generation in solid-state lasers," IEEE J. Sel. Top. Quantum Electron. **2**(3), 435–453 (1996).
22. U. Keller, "Recent developments in compact ultrafast lasers," Nature **424**(6950), 831–838 (2003).
23. M. Kuznetsov, F. Hakimi, R. Sprague, and A. Mooradian, "High-power (>0.5-W CW) diode-pumped vertical-external-cavity surface-emitting semiconductor lasers with circular TEM00 beams," IEEE Photonics Technol. Lett. **9**(8), 1063–1065 (1997).
24. S. Calvez, J. E. Hastie, M. Guina, O. G. Okhotnikov, and M. D. Dawson, "Semiconductor disk lasers for the generation of visible and ultraviolet radiation," Laser Photonics Rev. **3**(5), 407–434 (2009).
25. B. Rösener, N. Schulz, M. Rattunde, C. Manz, K. Köhler, and J. Wagner, "High-power high-brightness operation of a 2.25- m (AlGaIn)(AsSb)-based barrier-pumped vertical-external-cavity surface-emitting laser," IEEE Photonics Technol. Lett. **20**(7), 502–504 (2008).
26. D. J. M. Stothard, J.-M. Hopkins, D. Burns, and M. H. Dunn, "Stable, continuous-wave, intracavity, optical parametric oscillator pumped by a semiconductor disk laser (VECSEL)," Opt. Express **17**(13), 10648–10658 (2009).
27. J. D. Berger, D. W. Anthon, A. Caprara, J. L. Chilla, S. V. Govorkov, A. Y. Lepert, W. Mefferd, Q.-Z. Shu, and L. Spinelli, "20 Watt CW TEM00 intracavity doubled optically pumped semiconductor laser at 532 nm," SPIE Proceedings **8242**, 824206 (2012).
28. H. Kahle, R. Bek, M. Heldmaier, T. Schwarzbäck, M. Jetter, and P. Michler, "High optical output power in the UVA range of a frequency-doubled, strain-compensated AlGaInP-VECSEL," Appl. Phys. Express **7**(9), 092705 (2014).
29. S. Hoogland, S. Dhanjal, A. C. Tropper, S. J. Roberts, R. Häring, R. Paschotta, F. Morier-Genoud, and U. Keller, "Passively mode-locked diode-pumped surface-emitting semiconductor laser," IEEE Photonics Technol. Lett. **12**(9), 1135–1137 (2000).
30. U. Keller and A. C. Tropper, "Passively modelocked surface-emitting semiconductor lasers," Phys. Rep. **429**(2), 67–120 (2006).
31. K. G. Wilcox, A. C. Tropper, H. E. Beere, D. A. Ritchie, B. Kunert, B. Heinen, and W. Stolz, "4.35 kW peak power femtosecond pulse mode-locked VECSEL for supercontinuum generation," Opt. Express **21**(2), 1599–1605 (2013).
32. P. Klopp, U. Griebner, M. Zorn, and M. Weyers, "Pulse repetition rate up to 92 GHz or pulse duration shorter than 110 fs from a mode-locked semiconductor disk laser," Appl. Phys. Lett. **98**(7), 071103 (2011).
33. C. A. Zaugg, A. Klenner, M. Mangold, A. S. Mayer, S. M. Link, F. Emaury, M. Golling, E. Gini, C. J. Saraceno, B. W. Tilma, and U. Keller, "Gigahertz self-referenceable frequency comb from a semiconductor disk laser," Opt. Express **22**(13), 16445–16455 (2014).
34. M. Mangold, M. Golling, E. Gini, B. W. Tilma, and U. Keller, "Sub-300-femtosecond operation from a MIXSEL," Opt. Express **23**(17), 22043–22059 (2015).
35. M. Mangold, S. M. Link, A. Klenner, C. A. Zaugg, M. Golling, B. W. Tilma, and U. Keller, "Amplitude noise and timing jitter characterization of a high-power mode-locked integrated external-cavity surface emitting laser," IEEE Photonics J. **6**(1), 1–9 (2014).

#253662 Received 9 Nov 2015; revised 18 Jan 2016; accepted 19 Jan 2016; published 25 Jan 2016

36. G. Baili, L. Morvan, M. Alouini, D. Dolfi, F. Bretenaker, I. Sagnes, and A. Garnache, "Experimental demonstration of a tunable dual-frequency semiconductor laser free of relaxation oscillations," Opt. Lett. **34**(21), 3421–3423 (2009).
37. S. De, G. Baili, S. Bouchoule, M. Alouini, and F. Bretenaker, "Intensity- and phase-noise correlations in a dual-frequency vertical-external-cavity surface-emitting laser operating at telecom wavelength," Phys. Rev. A **91**(5), 053828 (2015).
38. U. Keller, T. H. Chiu, and J. F. Ferguson, "Self-starting and self-Q-switching dynamics of passively mode-locked Nd:YLF and Nd:YAG lasers," Opt. Lett. **18**(3), 217–219 (1993).
39. C. Hönninger, R. Paschotta, F. Morier-Genoud, M. Moser, and U. Keller, "Q-switching stability limits of continuous-wave passive mode locking," J. Opt. Soc. Am. B **16**(1), 46–56 (1999).
40. A. Joshi and S. Datta, "Dual InGaAs photodiodes having high phase linearity for precise timing applications," IEEE Photonics Technol. Lett. **21**(19), 1360–1362 (2009).
41. V. J. Wittwer, R. van der Linden, B. W. Tilma, B. Resan, K. J. Weingarten, T. Sudmeyer, and U. Keller, "Sub-60-fs timing jitter of a SESAM modelocked VECSEL," IEEE Photonics J. **5**(1), 1400107 (2013).
42. U. Keller, K. D. Li, M. J. W. Rodwell, and D. M. Bloom, "Noise characterization of femtosecond fiber raman soliton lasers," IEEE J. Quantum Electron. **25**(3), 280–288 (1989).
43. R. Paschotta and U. Keller, "Passive mode locking with slow saturable absorbers," Appl. Phys. B **73**(7), 653–662 (2001).

1. Introduction

A modelocked laser can support not only very short pulses but at the same time very precise frequency metrology for the most accurate clocks. These ultrafast – or ultra-short pulse – lasers are dramatically impacting many areas of photonics, from basic science to industrial manufacturing and biomedicine. The design and performance of the lasers behind these applications is critical for new discoveries, creating new applications and opening new market opportunities. Modelocked lasers produce a frequency comb for which the frequency spacing (i.e. the pulse repetition rate) has been stabilized in the 1980th [1,2] achieving close to quantum-noise limited performance with diode-pumped solid-state lasers [3]. However the stabilization of the frequency comb offset (i.e. the carrier envelope offset (CEO) frequency) remained a challenge and only has become possible more recently [4–6]. Since then the field of optical frequency combs has evolved very quickly, and current applications range from high-precision spectroscopy [7,8] over frequency metrology [4,9] to ultra-high-speed optical communication [10,11]. Many of these applications are based not only on one, but on two frequency combs such as dual-comb spectroscopy [12–16], asynchronous optical sampling (ASOPS) [17], pump probe measurements and fiber Bragg grating sensing [18]. Usually two separate lasers need to be stabilized and therefore, one simple, compact and cost-efficient dual-comb laser would be greatly beneficial for these kind of applications.

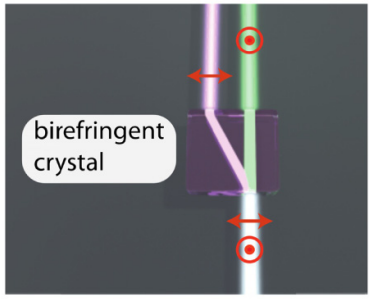

Fig. 1. A birefringent crystal splits an unpolarized beam into two orthogonally polarized beams which are collinear but spatially separated with different optical path lengths in the birefringent crystal.

We have introduced the concept of dual-comb lasers [19] to generate two modelocked beams with slightly different pulse repetition rates using only a single gain medium in a shared cavity. The dual-comb emission is obtained by inserting a birefringent crystal into the laser cavity, to split an unpolarized cavity-beam into two cross-polarized beams, which are

#253662 Received 9 Nov 2015; revised 18 Jan 2016; accepted 19 Jan 2016; published 25 Jan 2016

collinear but spatially separated and have slightly different optical path lengths in the birefringent crystal (Fig. 1). The pulse repetition rate is set by the cavity length and the difference by the different optical path length inside the birefringent crystal (Fig. 1) that can be adjusted by the crystal thickness and even compensated using a second birefringent crystal. For the first dual-comb laser demonstration [19] we used an optically pumped semiconductor laser, referred to as the modelocked integrated external-cavity surface emitting laser (MIXSEL) [20], which integrates the saturable absorber of a semiconductor saturable absorber mirror (SESAM) [21,22] with the gain structure of a vertical external-cavity surface emitting laser (VECSEL) [23] into a single semiconductor wafer. Thus modelocking in a simple straight linear cavity can be achieved with a MIXSEL (Fig. 2). VECSELs and MIXSELs are part of the family of optically pumped semiconductor disk lasers and have become successful industrial products due to their large spectral range of operation from the infrared to the visible [24–26] and even reaching the UV regime [27,28]. Passively modelocked VECSELs first demonstrated in 2000 [29,30] using SESAMs have been improved to peak power levels of up to 4.35 kW [31] and pulses as short as 107 fs [32]. The potential of optically pumped semiconductor disk lasers for the generation of low-noise frequency combs has been demonstrated using a SESAM-modelocked VECSEL, however, at this point still with the additional complexity of external pulse amplification and compression to obtain the required peak power for frequency comb stabilization [33].

More recent progress with MIXSELs results in pulse durations as short as 253 fs with 240 W of peak power [34]. The reduced complexity in comparison to any diode-pumped ultrafast solid-state laser makes the MIXSEL platform very attractive and particularly interesting for dual-comb lasers. The first demonstration of a dual-comb MIXSEL [19] generated two modelocked pulse trains with an average output power per beam of around 70 mW, pulse durations of 13 ps and 19 ps and a pulse repetition rate of 1.890 GHz and 1.895 GHz, respectively.

A single-comb MIXSEL with actively stabilized pulse repetition frequency has shown excellent noise performance with record–low timing jitter for the arrival time of the pulses [35]. A dual-comb MIXSEL (Fig. 1 and 2), however, revealed an initially very surprising result: when the cavity length was corrected by the error signal of one beam only, the other beam was not affected significantly (i.e. the timing jitter noise was uncorrelated). This means that the pulse repetition rates of the two cross-polarized beams seem to be decoupled from each other even though they share all components within the linear cavity (Fig. 2).

In this paper we will explain the observed uncorrelated timing jitter noise of the two frequency combs (Fig. 3) and provide a solution how to stabilize both pulse repetition frequencies at the same time (Fig. 4). To explore the underlying physics we studied both a semiconductor and Nd:YAG dual-comb laser with opposite gain parameters in terms of upper state lifetimes (nanoseconds versus 230 μs) and gain cross sections ($\approx 10^{-14}$ cm^2 versus 2.8 x 10^{-19} cm^2) using in both cases the same pump laser diodes and the same intracavity birefringent crystals. For the dual-comb Nd:YAG laser (Fig. 5) we used a separate SESAM as one end-mirror of the linear folded cavity which allowed us to have perfect beam overlap in the gain. The outcome was that the spatially and temporarily incoherent pump laser was not responsible for the uncorrelated noise observed with the dual comb MIXSEL because we observed the same behavior with the dual comb Nd:YAG laser using the same pumping schemes. Furthermore with the dual-comb Nd:YAG laser as shown in Fig. 5 we could separate the two beams on the SESAM alone. This gave us strong experimental evidence that the noise of both beams is uncorrelated due to the time delay, that is introduced by the saturated SESAM since only the leading edge of the pulse experiences absorption. This was further confirmed when the difference in pulse repetition rates was reduced to allow for sufficient temporal overlap of the two pulses on the SESAM. At a certain point for these small differences the two pulse repetition rates have become locked as long as we provide some partial spatial beam overlap on the SESAM. Furthermore, with an increasingly larger spatial

#253662 Received 9 Nov 2015; revised 18 Jan 2016; accepted 19 Jan 2016; published 25 Jan 2016

overlap of the two beams on the SESAM, the modelocking has become only stable for one beam because of net-gain competition between the two beams due to small inhomogeneities in the birefringent crystal and SESAM.

For all cases we were able to finally stabilize both frequency combs. For applications such as high-precision spectroscopy we need the stabilization of both the pulse repetition frequency f_{rep} (i.e. comb spacing) and of the carrier envelope offset (CEO) frequency f_{CEO} (i.e. comb offset). The stabilization of the pulse repetition frequency of one of the beams enables for the first time to observe the effect on the phase noise of the other beam that shares the same cavity.

In the next sections we describe in more details the two different dual comb lasers and their noise characterizations. Our dual comb modelocked laser was initially motivated by the dual frequency VECSEL [36], where the VECSEL is operated in continuous wave (cw). A recent study of noise correlation in such dual-frequency VECSELs [37] could be interesting for the "locked" regime of operation where both beams have the same pulse repetition rate. However, for dual comb spectroscopy applications we need two different pulse repetition rates and our focus in this paper is with regards to the origin of the decoupled timing jitter noise between the two output beams with different pulse repetition rates. We test our observation for two lasers, an optically pumped MIXSEL and Nd:YAG laser, using the same pump laser and the same SESAM for modelocking. These lasers operate in different regimes of noise properties [35,38,39] with strong relaxation oscillations, long upper state lifetimes and small gain cross sections in the latter case, but show very similar behavior with regards to the uncorrelated timing jitter.

2. Phase noise of the dual-comb MIXSEL

For the dual-comb MIXSEL (Fig. 2) we have a simple straight linear cavity defined by the MIXSEL chip and the output coupler (OC) as the two end mirrors. In this case it is straightforward to apply the concept of polarization-duplexing with a $CaCO_3$ birefringent crystal inside the laser cavity, splitting the one cavity beam into two spatially separated and orthogonally polarized beams with slightly different pulse repetition frequencies of 1.895 GHz and 1.890 GHz [19]. The center wavelength of the two beams also slightly differs with 966.11 nm and 966.01 nm, but their spectra are still well overlapping within the full width at half maximum of 0.25 nm and 0.23 nm for the s- and the p-polarized beam, respectively. The pulse duration for the s-polarized beam is 13.5 ps and for the p-polarized beam 19.1 ps and the average output power of each beam is ≈70 mW. These modelocking parameters slightly vary for the different configurations tested within this paper. More details on the cavity and the modelocking performance can be found in [19].

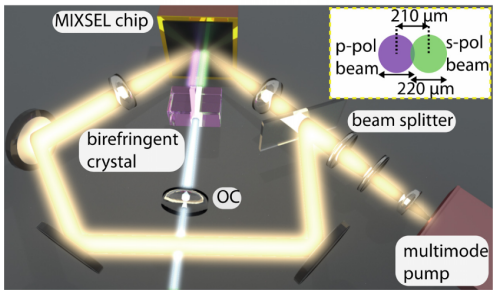

Fig. 2. Dual-comb MIXSEL setup: the linear straight laser cavity is defined by the MIXSEL chip and output coupler (OC). An intracavity birefringent crystal is introduced to generate two beams (Fig. 1). The MIXSEL is pumped with a multi-mode semiconductor diode array which is split with a 50:50 beam splitter such that both cavity modes on the MIXSEL chip can be pumped under an angle of 45°. Inset: the two cavity modes on the MIXSEL chip with a diameter of 220 µm, separated by 210 µm with a small overlap

#253662 Received 9 Nov 2015; revised 18 Jan 2016; accepted 19 Jan 2016; published 25 Jan 2016

The phase noise of the s- and p-polarized beam is measured in free-running and stabilized operation with a commercial signal source analyzer (SSA) (Agilent E5052B). The two collinear output beams are separated with a polarizing beam splitter (PBS) (Fig. 3), and each beam is independently fiber coupled and either the s-or the p-polarized beam is detected by a highly linear photodiode (PD1) (HLPD, Discovery Semiconductors Inc. DSC30S [40]). For the stabilization of the pulse repetition frequency, again part of either the s- or p-polarized beam is detected with a photodetector (PD2) (Thorlabs, DET01CFC) and then mixed in a double balanced mixer with a signal from a low noise electronic reference. The resulting phase error signal is then filtered with a custom designed proportional-integral loop filter [41] and the feedback of this phase-locked loop (PLL 1) is sent to the piezo-controlled output coupler to adjust the dual-comb laser cavity length. The PLL is adapted from previous pulse repetition frequency stabilizations of a MIXSEL [35].

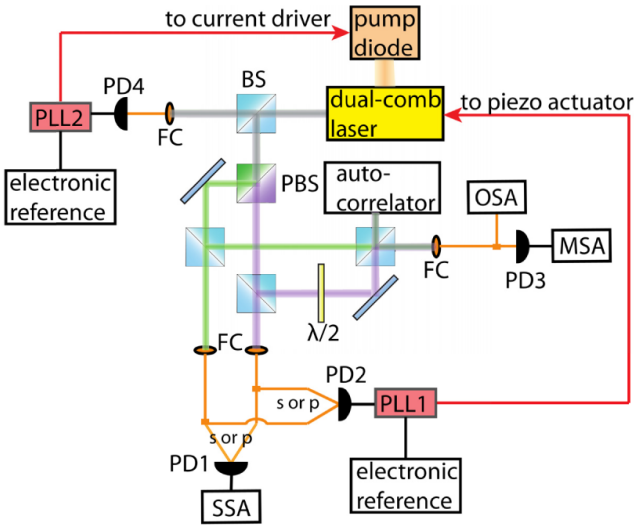

Fig. 3. Laser characterization: each beam is characterized with a second harmonic autocorrelation, an optical spectrum analyzer (OSA), a microwave spectrum analyzer (MSA) and a signal source analyzer (SSA, Agilent E5052B). Two feedback loops can be applied. The first phase-locked loop (PLL1) gives a feedback of the error signal of one of the pulse repetition rates on the piezo-controlled output coupler to adjust the cavity length (i.e. for either the s or p polarized beam). The second phase-locked loop (PLL2) detects the interference of the two beams and gives a feedback of the error signal of the difference in pulse repetition rate on the current driver of the multimode pump; BS: beam splitter, PBS: polarizing beam splitter, FC: fiber coupling, PD: photodetector, λ/2: lambda half-wave plate

The phase noise measurement with the SSA shows a noise reduction of over 100 dB for the s-polarized beam (Fig. 4(a)) from free-running operation (turquoise line) to the case of actively stabilizing the error signal of the s-polarized beam (green line). Turning on the active stabilization of the p-polarized beam and at the same time measuring the phase noise of the s-polarized beam (blue line), shows that the stabilization of the p-polarized beam has in comparison no significant influence on the s-polarized beam. The same applies for the phase noise measurement of the p-polarized beam (Fig. 4(b)).

#253662 Received 9 Nov 2015; revised 18 Jan 2016; accepted 19 Jan 2016; published 25 Jan 2016

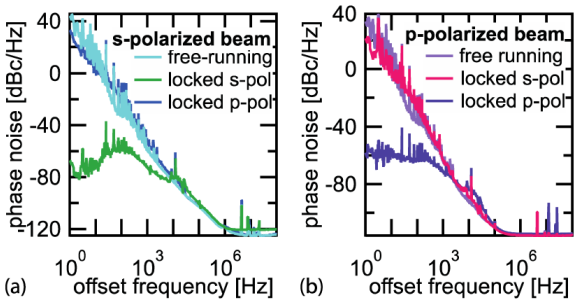

Fig. 4. Dual-comb MIXSEL: power spectral densities of the measured timing phase noise for the arrival time of the pulses in each frequency comb [42] using a commercial signal source analyzer (SSA – Agilent E5052B) for the (a) s-polarized beam and for the (b) p-polarized beam, both in free-running operation, and with a feedback given on the error of the s-polarized beam (locked s-pol) or on the error of the p-polarized beam (locked p-pol). The vertical axis shows phase noise in units of dBc per hertz bandwidth: decibels relative to carrier i.e. dB below pulse repetition rate peak signal. The phase noise of both beams is uncorrelated. The integrated timing jitter over the whole measurement span from 1 Hz to 100 MHz is in case of the s-polarized beam reduced by more than 3 orders of magnitude from 16.5 ns in free-running operation to 4.3 ps with active stabilization of the s-polarized beam. Same applies for the p-polarized beam with a reduction from 8 ns free-running to 4.8 ps with active feedback on the p-polarized beam.

This uncorrelated timing jitter for the two frequency combs (Fig. 4) has initially been a surprise, since both beams share the same cavity and the feedback moves the output coupler for both beams. This implicates that the feedback of the stabilization is not only compensating mechanical vibrations of the cavity but accounts also for a noise source that is not common for both beams. We wanted to explore the most likely sources for these decoupled noise such as time delay on the saturable absorber [43] and pump laser noise.

We used a low-coherent multi-mode diode array laser to pump the MIXSEL. The short nanosecond upper-state lifetime of the semiconductor gain-material could potentially make the dual-comb MIXSEL more susceptible to the pump laser noise because the two cavity beams on the MIXSEL chip were both pumped under an angle of 45 degrees by splitting the pump beam with a 50:50 beam splitter (Fig. 2). Therefore, there is a spatial and temporal difference for the pump at the two spots on the gain. To explore this further we build a second dual comb laser using a Nd:YAG gain crystal with an upper state lifetime of 230 µs. The results with this laser are explained in more details in the next section.

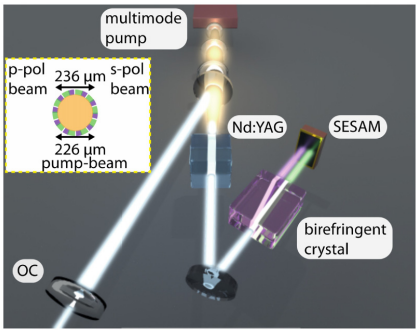

Fig. 5. Dual-comb Nd:YAG laser setup: the cavity comprises (from left to right) an output coupler (OC), a flat dichroic folding mirror, the Nd:YAG crystal, a curved folding mirror to focus on the SESAM, the birefringent $CaCO_3$ crystal and the SESAM. The pump beam is focused through the dichroic folding mirror into the Nd:YAG crystal. Inset: The s- and p-polarized beams are perfectly overlapping in the Nd:YAG crystal with a beam diameter of 236 µm and a slightly smaller pump diameter of 226 µm.

#253662 Received 9 Nov 2015; revised 18 Jan 2016; accepted 19 Jan 2016; published 25 Jan 2016

3. Nd:YAG dual-comb

With a dual-comb Nd:YAG laser (Fig. 5) we need to separate the gain and absorber in two cavity elements which allows us to pump the gain for both combs fully overlapping in the gain. In this case both combs are pumped under identical conditions and the two beams are only separated on the SESAM. This will decouple the two most probable timing jitter noise sources. In addition the much longer upper state lifetime of the Nd:YAG laser (230 µs versus nanoseconds) would reduce any possible pump noise induced timing jitter observed in the MIXSEL. The birefringent crystal is inserted in front of the SESAM (Fig. 5), such that the two cavity beams are spatially separated on the saturable absorber alone and perfectly overlap in the gain. With this configuration, the same geometry for the pump beam can be used to pump both beams simultaneously (Fig. 5(inset)). The diameter of the pump beam is chosen slightly smaller (226 µm) than the diameter of the two cavity beams (236 µm) to insure a good TEM_{00} beam profile. The M^2 value is measured to be 1.1 or smaller for both beams in x- and y-direction (Fig. 6 (a) and (b)). We used the same pump laser as before with the MIXSEL and a 1% output coupler. The modelocking performance of both beams is nearly identical in terms of beam profile, optical spectrum and pulse duration (Fig. 6). The average output power is 400 mW and 530 mW for the s- and p-polarized beam, respectively.

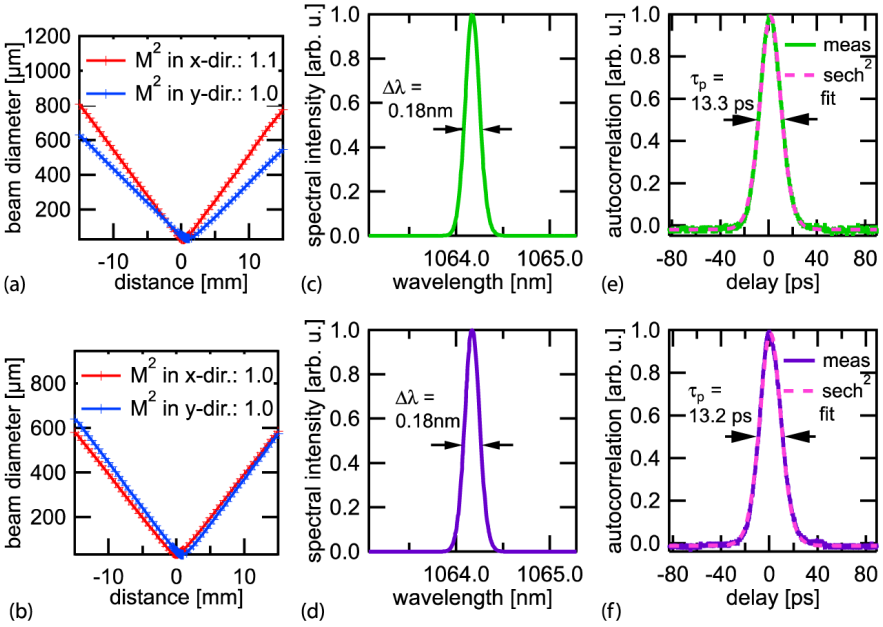

Fig. 6. Dual-comb Nd:YAG laser: Beam profile M2 measurements of the (a) s-polarized beam and of the (b) p-polarized beam. Optical spectrum of the (c) s-polarized beam and of the (d) p-polarized beam, both centered at 1064.5 nm. Second harmonic autocorrelation of the (e) s-polarized beam and of the (f) p-polarized beam revealing a pulse duration of around 13 ps.

The dual comb performance is similar as observed before with the MIXSEL [19]. We measured the microwave spectrum of the optical interference signal of the two combs on a fast photodetector (PD3) (NewFocus Model 1414) (Fig. 3). Optical interference is achieved when we turn the polarization of the p-polarized beam by 90 degrees with a lambda half-wave plate (λ/2) after passing the first beam splitter (BS) and then recombine with the s-polarized beam. The output signal of PD3 is shown on a microwave spectrum analyzer (MSA) between DC and the pulse repetition frequencies in a span of 1.2 GHz and a resolution bandwidth (RBW) of 10 kHz (Fig. 7(a)). A decreased span of 10 MHz in a RBW of 3 kHz (Fig. 7(b))

#253662 Received 9 Nov 2015; revised 18 Jan 2016; accepted 19 Jan 2016; published 25 Jan 2016

shows that the difference in pulse repetition frequencies (Δf_{rep}), due to the different optical path-lengths in the birefringent crystal, is around 2.35 MHz. The difference frequency Δf_{rep} appears also as additional side-peaks around DC and the pulse repetition frequencies. Very interesting for applications, for example for dual-comb spectroscopy, is the comb structure ($comb_1$) in between DC and the pulse repetition rates (Fig. 7(a)). In a reduced span of 200 MHz and a RBW of 10 kHz, the individual comb lines are visible, which are spaced by Δf_{rep} (Fig. 7(c)). This comb is only visible, if we observe optical interference of both beams on PD 3. This comb represents a direct link between the optical terahertz frequencies and the electronically accessible microwave regime.

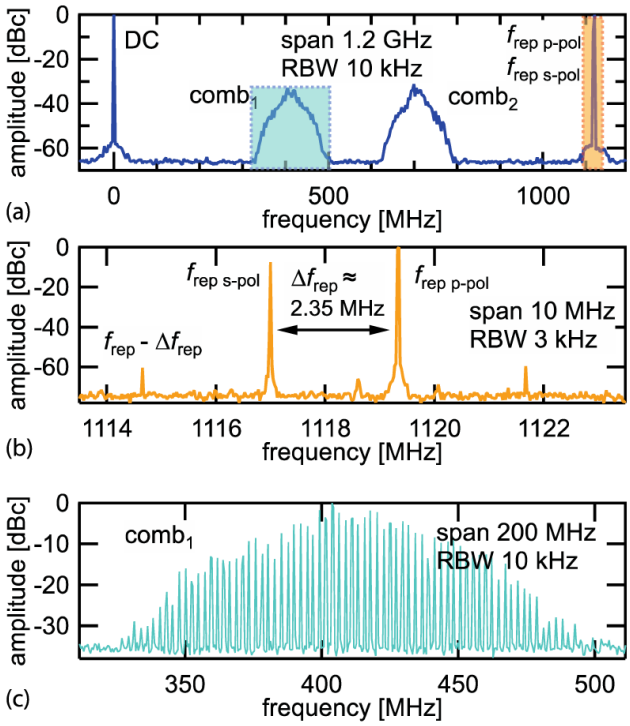

Fig. 7. Dual-comb Nd:YAG laser with a 3-mm-thick birefringent plate (Fig. 5): (a) microwave spectrum analyzer (MSA) signal from DC to 1.2 GHz with a resolution bandwidth (RBW) of 10 kHz. (b) Zoom-in around the pulse repetition frequencies with a span of 10 MHz and a RBW of 3 kHz. (c) Zoom-in around the first comb ($comb_1$) with a span of 200 MHz and a RBW of 10 kHz.

4. Noise correlation study

We use the same timing jitter characterization configuration (Fig. 3) and observe the same uncorrelated timing jitter between the two beams (Fig. 8) as before with the dual-comb MIXSEL (Fig. 4). Therefore, we can conclude that the pump noise is not the source for the uncorrelated timing jitter of the two beams.

#253662 Received 9 Nov 2015; revised 18 Jan 2016; accepted 19 Jan 2016; published 25 Jan 2016

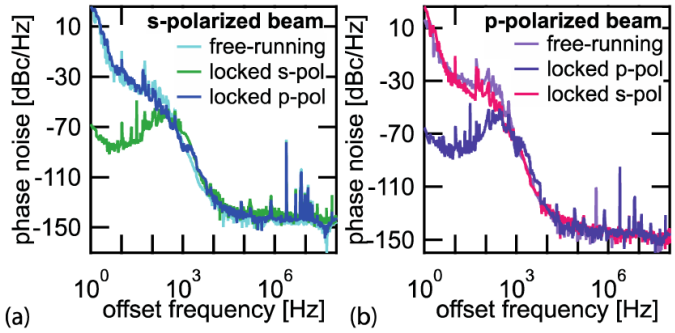

Fig. 8. Dual-comb Nd:YAG laser: power spectral densities of the measured timing phase noise for the arrival time of the pulses in each frequency comb [42] using a commercial signal source analyzer (SSA – Agilent E5052B) for the (a) s-polarized beam and for the (b) p-polarized beam, both in free-running operation, and with a feedback given on the error of the s-polarized beam (locked s-pol) or on the error of the p-polarized beam (locked p-pol). The phase noise of both beams is uncorrelated as before with the dual-comb MIXSEL (Fig. 4). The integrated timing jitter over the whole measurement span from 1 Hz to 100 MHz is in case of the s-polarized beam reduced again by nearly 3 orders of magnitude from 2 ns in free-running operation to 6.4 ps with active stabilization of the s-polarized beam. Same applies for the p-polarized beam with a reduction from 856 ps free-running to 5.8 ps with active feedback on the p-polarized beam.

We used the dual-comb lasers for further parameter studies that are summarized in Table 1. The Nd:YAG laser allows for studies with beam overlap on the SESAM independent of the overlap on the gain. In configuration number 1 and 2, Δf_{rep} between the two perpendicularly polarized output combs is in the megahertz range.

Table 1. Overview of the different laser configurations used in this paper

configuration	1	2	3	4	5	6	7
laser	MIXSEL	Nd:YAG	Nd:YAG	Nd:YAG	MIXSEL	MIXSEL	MIXSEL
same pump configuration	✗	✓	✓	✓	✗	✗	✗
overlap on gain	partly	full	full	full	partly	partly	partly
overlap on saturable absorber	partly	✗	partly	✗	partly	partly	partly
feedback on $f_{rep,1}$ via piezo	✓	✓	✗	✗	✓	✓	✗
Δf_{rep}	5 MHz	2.5 MHz	0 Hz	88 kHz	0 Hz	5 MHz	5 MHz
feedback on Δf_{rep} via pump-current	✗	✗	✗	✗	✗	✓	✓
passive locking of pulse repetition rate	✗	✗	✓	✗	✓	✗	✗
stabilization of $f_{rep,1}$ and $f_{rep,2}$	✗	✗	✗	✗	✓	✓	✗

In a configuration number 3 (Table 1) with the dual-comb Nd:YAG laser we have inserted a second intracavity birefringent crystal with the same thickness of 1 mm but with the optical axis rotated by 90 degrees such that both beams have approximately the same optical path length inside the cavity (Fig. 9(a)). We still maintain a small spatial overlap of the two beams on the SESAM (Fig. 9(b)) but now in addition we also allow for a temporal overlap of the two pulses. The microwave spectrum of the two superimposed beams is measured again in the same polarization (Fig. 10(a)). Between DC and the pulse repetition rate there is in this case only a single strong signal left instead of the previous microwave comb structure ($comb_1$ in Fig. 7). The repetition rate of the two beams is exactly the same (Δf_{rep} = 0 Hz), because passive locking of the pulse repetition rate occurs between the two beams with the additional temporal overlap. Therefore, the only difference in their frequency combs is the carrier envelope offset frequencies, and the measured signal is the relative carrier envelope offset Δf_{CEO} with a signal to noise ratio of more than 40 dB (Fig. 10(b)).

#253662 Received 9 Nov 2015; revised 18 Jan 2016; accepted 19 Jan 2016; published 25 Jan 2016

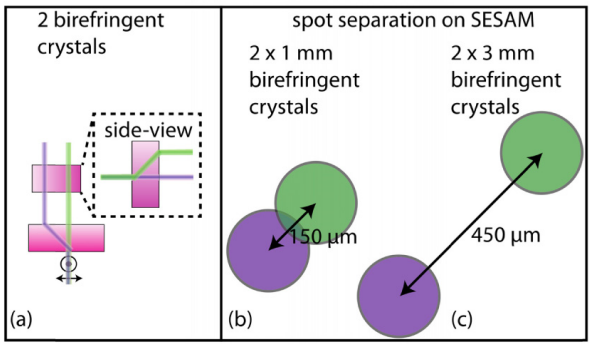

Fig. 9. (a) Insertion of a second birefringent crystal of same thickness but with the optical axis rotated by 90°, such that both beams have approximately the same optical path length. (b) In configuration number 3 (Table 1), the beams overlap slightly on the SESAM with a distance between the centers of the two beams of ≈150 µm. The beam diameter is for both beams ≈ 180 µm. (c) In configuration number 4 (Table 1) the distance between the beams on the SESAM is increased to ≈450 µm, such that there is no overlap between the beams.

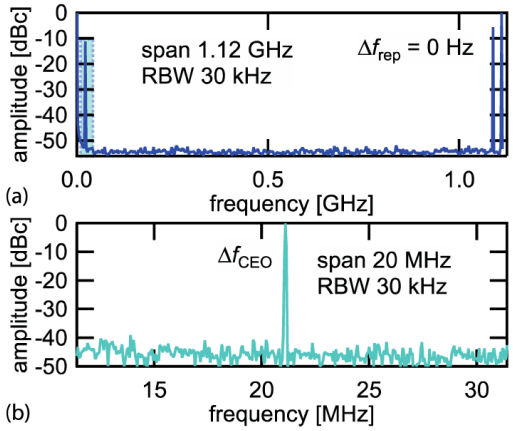

Fig. 10. Dual-comb Nd:YAG laser with two 1-mm-thick birefringent crystals (Fig. 9(a)) to sufficiently reduce the different optical cavity length of the two beams to passively lock the two pulse repetition rates: (a) Microwave spectrum analyzer (MSA) signal from DC to 1.12 GHz. Both beams have exactly the same pulse repetition frequency due to passive locking of two overlapping pulses in the saturable absorber (Fig. 9(b)). Therefore, the only difference in frequency between the two beams is the carrier envelope offset (CEO) frequency. (b) Instead of a comb structure ($comb_1$ in Fig. 7) we observe only one single strong frequency signal which is the relative CEO frequency (Δf_{CEO}) between the two combs.

To further confirm our conclusions from configuration number 3 we studied configuration number 4 for which we increased the beam separation to obtain no pulse overlap on the SESAM (Fig. 9(c)). In this case we used two birefringent crystals of 3 mm thickness. Sure enough we did not observe the passive locking of the pulse repetition rate (Fig. 11(a)). A zoom-in on the signal between DC and the repetition rates (Fig. 11(b)) reveals again a comb structure with a comb-line spacing of 88 kHz, which is the difference in pulse repetition rate.

#253662 Received 9 Nov 2015; revised 18 Jan 2016; accepted 19 Jan 2016; published 25 Jan 2016

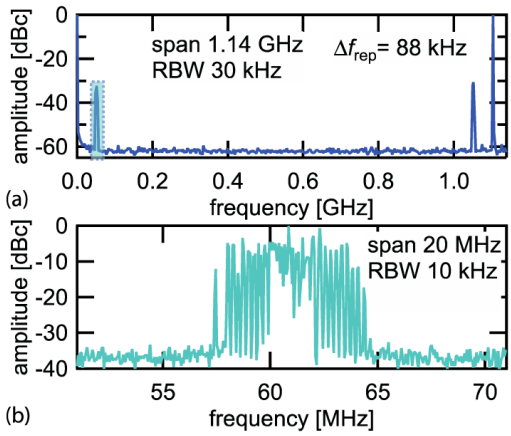

Fig. 11. Dual-comb Nd:YAG laser with two 3-mm-thick birefringent crystals (Fig. 9(c)) to obtain no spatial beam overlap on the SESAM but still with significant temporal overlap: (a) microwave spectrum analyzer (MSA) signal from DC to 1.14 GHz. The difference in pulse repetition frequency (Δf_{rep}) is 88 kHz since no passive pulse repetition rate locking occurs because the beams do not overlap on the saturable absorber. (b) Zoom-in around the first comb with a span of 20 MHz and a RBW of 10 kHz. The comb-line-spacing is reduced to 88 kHz, because it is set by Δf_{rep}.

In configuration number 5 we measure the timing phase noise of both beams with active stabilization under the condition of passive locking of the pulse repetition rate (i.e. with two intracavity birefringent crystals (Fig. 9(a)). With the Nd:YAG laser, the SESAM modelocking is, however, at its stability limit due to the increased loss of the two birefringent plates at gigahertz pulse repetition rates. We therefore continued with the MIXSEL which does not suffer from Q-switching instabilities. The phase noise measurement (Fig. 12(a) and 12(b)) shows, that the s-polarized and the p-polarized beam are stabilized simultaneously, independent of the specific beam used for the feedback control. Thus with partial pulse overlap on the MIXSEL chip the timing phase noise becomes correlated. They are both stabilized simultaneously, however the pulse repetition frequency is also the same for both beams. Typically however, for most applications two different but still stabilized pulse repetition rates are required.

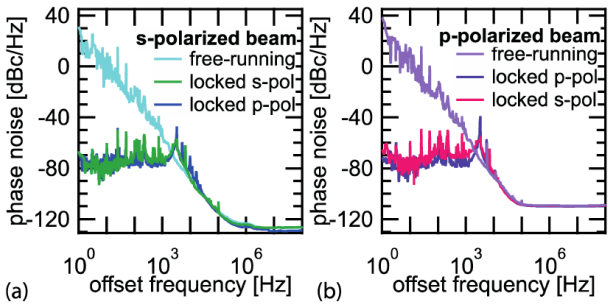

Fig. 12. Timing phase noise of a dual-comb MIXSEL with two intracavity 1-mm-thick birefringent crystals (Fig. 9(a)) with partial pulse overlap on the MIXSEL chip: (a) s-polarized beam and (b) p-polarized beam, both in free-running operation and with a feedback given on the error of the s-polarized beam (locked s-pol) or on the error of the p-polarized beam (locked p-pol). The phase noise of both beams is correlated.

For a strongly saturated absorber only the leading edge of the pulse experiences absorption which introduces an effective pulse delay (Fig. 13(a)) [43]. For our laser the incident pulse

#253662 Received 9 Nov 2015; revised 18 Jan 2016; accepted 19 Jan 2016; published 25 Jan 2016

fluence on the saturable absorber is more then 10-times larger than the saturation fluence of the absorber. This means that the pulse is shifted back in time with each roundtrip. The estimated pulse delay is in the order of 10 fs for a pulse duration of around 13 ps (Eq. (9) in [43]). This delay is not the same for both pulse trains, because it depends on the energy in each pulse and of course also on the saturable absorber. Small inhomogeneity in SESAM and MIXSEL will result in slightly different time delays and also explained the slightly different pulse performance in the two beams before [19]. However if the difference in roundtrip time is in the order of the saturation-induced pulse delay (e.g. for configuration number 3 in Tab. 1 a Δf_{rep} = 88 kHz results in a difference in roundtrip time of $\Delta T_{rt} \approx 70$ fs) we could observe passive locking of the pulse repetition rate when the two beams also have a partial spatial overlap. If Δf_{rep} is in the megahertz range, ΔT_{rt} is in the picosecond range and therefore orders of magnitude larger than the saturation-induced pulse delay and no passive locking of the pulse repetition rate occurs.

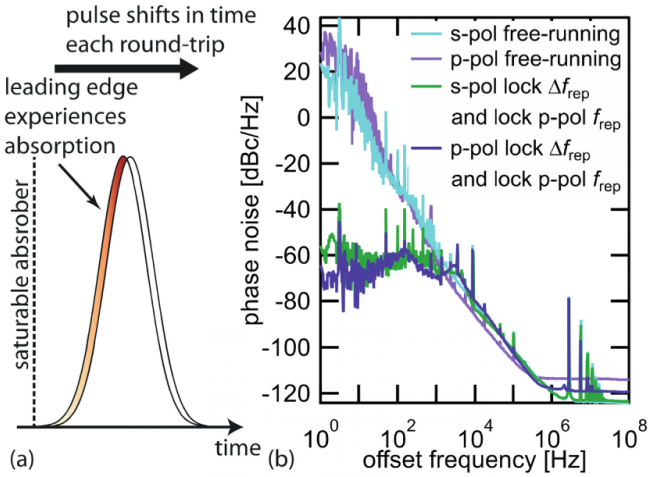

Fig. 13. (a) Strongly saturated absorber introduces a pulse delay with each round-trip, because only the leading edge of the pulse experiences absorption since the absorber is already saturated for the trailing edge of the pulse. (b) Timing phase noise of the MIXSEL (Fig. 2) with only one birefringent crystal without pulse overlap in the MIXSEL chip. Both beams can only be stabilized simultaneously when two feedback loops are applied (Fig. 3).

For the dual-comb MIXSEL we therefore can only obtain stabilization of two different pulse repetition rates in the megahertz regime (i.e. with only one birefringent crystal as shown in Fig. 2) when we apply two feedback loops to stabilize the two uncorrelated noise sources. We can achieve this for a case with $\Delta f_{rep} \approx 5$ MHz when we use one feedback loop (PPL1 in Fig. 3) to adjust the cavity length based on the error signal of one beam and a second feedback loop (PPL2 in Fig. 3) to adjust the pump power on the error signal of the difference of the pulse repetition rates (configuration number 6 in Table 1). In contrast to the microwave comb structure, which is a result of the optical interference of the two optical beams and can only be detected if both beams are superimposed in the same polarization, the detection of the difference in pulse repetition rate is independent of the polarization and can also be detected if the beams are cross-polarized. The difference in pulse repetition rate is then isolated using a low pass filter, and the signal is mixed with a low noise electronic reference signal.

The measurement of the timing phase noise shows, that if both feedback loops are activated, both beams are stabilized for either using the s- or p-polarized beam for PPL1 (Fig. 13(b)). The feedback loop on the difference in pulse repetition frequencies accounts for the different pulse delays in the saturable absorber of the two beams. It is however not sufficient

#253662 Received 9 Nov 2015; revised 18 Jan 2016; accepted 19 Jan 2016; published 25 Jan 2016

for the stabilization of the two beams to turn on only PLL2 (configuration number 7 in Table 1), because it only locks the phase noise of one beam to the noise of the other beam. Only if additionally PLL1 is turned on, both beams are stabilized.

5. Conclusion and outlook

We have successfully demonstrated dual-comb lasers for both optically pumped semiconductor and Nd:YAG gain materials. An intracavity SESAM is used for passive modelocking and an intracavity birefringent filter is used to generate two collinear perpendicularly polarized output beams providing two frequency combs with two different pulse repetition rates from a single laser cavity (i.e. polarization-duplexed dual-comb laser).

We have successfully stabilized the pulse repetition rates for both gigahertz frequency combs. We explained the initially surprising observation that we need two feedback loops to stabilize the timing jitter for both beams when the laser is operated with significantly different pulse repetition rates. The different pulse delays for both beams, introduced by the strongly saturated absorber are responsible for the uncorrelated timing jitter of the two beams. We observed this uncorrelated noise for two different dual-comb lasers with very different gain materials such as semiconductor and Nd:YAG in terms of upper state lifetime and gain cross section. In both cases we used the same multi-mode diode laser array for pumping. We could demonstrate that in both cases the pump laser was not responsible for the uncorrelated noise of the pulse repetition rate in the two beams.

We could show that passive locking of the pulse repetition rate becomes possible with sufficient spatial and temporal pulse overlap in the absorber. In this case we only needed to apply one feedback loop to stabilize both frequency combs because the passive locking results in exactly the same pulse repetition rates in both beams. In this regime we have direct access to the difference in the frequency comb offset without any f-to-2f interferometric techniques [4].

The next step will be a more detailed analysis of the noise and possible stabilization schemes of the relative carrier envelope offset frequency. The MIXSEL structure used in this experiment supported only picosecond pulses. The recent progress in femtosecond MIXSELs [34] will support a much broader optical bandwidth centered around 1030 nm. We are confident that in the near future gas-spectroscopy, for example on Acetylene, using a fully stabilized dual-comb MIXSEL will be presented, opening up this compact and inexpensive source for many applications in the field of frequency metrology, optical sensing and pump-probe experiments.

Acknowledgments

The authors acknowledge support of the technology and clean room facility FIRST of ETH Zurich for advanced micro- and nanotechnology. This work was financed by the Swiss Confederation Program Nano-Tera.ch, which was scientifically evaluated by the Swiss National Science Foundation (SNSF).

#253662 Received 9 Nov 2015; revised 18 Jan 2016; accepted 19 Jan 2016; published 25 Jan 2016